

# Federated Learning Architectures: A Performance Evaluation with Crop Yield Prediction Application

Anwasha Mukherjee<sup>a,b,\*</sup>, Rajkumar Buyya<sup>b</sup>

<sup>a</sup>*Department of Computer Science*

*Mahishadal Raj College, Mahishadal, West Bengal, 721628, India*

<sup>b</sup>*Cloud Computing and Distributed Systems (CLOUDS) Laboratory,*

*School of Computing and Information Systems,*

*The University of Melbourne, Victoria, 3052, Australia*

---

## Abstract

Federated learning has become an emerging technology for data analysis for IoT applications. This paper implements centralized and decentralized federated learning frameworks for crop yield prediction based on Long Short-Term Memory Network. For centralized federated learning, multiple clients and one server is considered, where the clients exchange their model updates with the server that works as the aggregator to build the global model. For the decentralized framework, a collaborative network is formed among the devices either using ring topology or using mesh topology. In this network, each device receives model updates from the neighbour devices, and performs aggregation to build the upgraded model. The performance of the centralized and decentralized federated learning frameworks are evaluated in terms of prediction accuracy, precision, recall, F1-Score, and training time. The experimental results present that  $\geq 97\%$  and  $> 97.5\%$  prediction accuracy are achieved using the centralized and decentralized federated learning-based frameworks respectively. The results also show that the using centralized federated learning the response time can be reduced by  $\sim 75\%$  than the cloud-only framework. Finally, the future research directions of the use of federated learning in crop yield prediction are explored in this paper.

*Keywords:* Federated learning, Prediction accuracy, Training time, Response time

---

## 1. Introduction

Agriculture is an important sector that has a huge impact on the economy of most of the countries. The conventional farming practices depend on manual decision making on crop harvesting, irrigation, etc., that suffers from improper selection of crops, inefficient utilization of lands, water resources, etc. To overcome these problems, smart agriculture and

---

\*Corresponding author

*Email addresses:* [anweshamukherjee2011@gmail.com](mailto:anweshamukherjee2011@gmail.com) (Anwasha Mukherjee),  
[rbuyya@unimelb.edu.au](mailto:rbuyya@unimelb.edu.au) (Rajkumar Buyya)

farming practices come into the scenario, where Internet of Things (IoT) plays a significant role (Debauche et al. ((2021)), Boursianis et al. ((2022))). In IoT-based smart agricultural systems, IoT devices are used for soil and environmental parameters' data collection, and then analysing the data for decision making (Bera et al. ((2023b,a))). For data analysis, machine learning (ML) and deep learning (DL) are used, and the cloud servers are used for storing and analysing the large volume of data. However, data storage and analysis inside the cloud requires huge amount of IoT data transmission to the cloud, that requires seamless network connectivity and high network bandwidth. However, the agricultural lands are mainly located at rural areas, where the network bandwidth may not be high, as well as seamless network connectivity may not available. Hence, data transmission from IoT devices to the cloud is a challenge. Further, the entire data transmission from IoT devices to the cloud cause high network traffic, and the storage and analysis of the huge volume of data increase the cloud overhead, latency, etc. To address these issues, edge computing and fog computing come (Bera et al. ((2023b, 2024))). In edge computing, the resources are placed at the edge of the network to reduce the latency and computation overhead on the cloud. In fog computing, the intermediate devices, e.g. switch, router, etc., process data to reduce the latency and overhead on the cloud. Nevertheless, the concern regarding data security and privacy still remains. Moreover, the soil data, environmental data, climate and weather conditions of various geographical regions are different, and the user may not like to transmit and store the data over the cloud due to privacy protection. Hence, personalized local models and an efficient global model are required to perform accurate prediction and utilize the agricultural resources efficiently. To utilize the edge devices for local data analysis and for collaborative training to develop a global model, federated learning (FL) (Nguyen et al. ((2021)), Zhang et al. ((2021)), Li et al. ((2020))) comes into the scenario.

FL is a learning approach that allows collaborative training with the coordination of multiple devices and a central server without sharing individual dataset (Nguyen et al. ((2021)), Mothukuri et al. ((2021))). In an edge-cloud-based FL, the edge devices serve as the clients and the cloud server acts as the central server, for collaborative training (Bera et al. ((2024))). In an FL-based framework (Nguyen et al. ((2021))), the central server serves as the aggregator that at first creates an initial global model with learning parameters. Each of the clients downloads the current model from the server, computes own model updates using its local dataset, and offloads the local update to the server. The server receives local updates from all clients, and develops an improved global model. The clients download the global update from the server, compute their local updates again, and offloads the updates to the server. This process is continued until the global training is finished. The principal advantages of FL are enhanced data privacy, low-latency, and learning quality enhancement (Nguyen et al. ((2021))). As no data is shared, privacy is protected (Mothukuri et al. ((2021)), Djenouri et al. ((2023))). Further, an enhanced version of the global model is created through collaborative training. As local data analysis takes place, the latency is reduced.

According to networking structure and data partitioning, the FL algorithms are classified into several categories. Based on data partitioning, FL algorithms are classified into three types (Nguyen et al. ((2021))): Vertical FL, Horizontal FL, and federated transfer learning.

In vertical FL systems, the clients have datasets with same sample space but different feature space. In horizontal FL systems, the clients have datasets with same feature space but different sample space. In federated transfer learning, the clients have datasets with different feature space as well as different sample space. According to the networking structure, FL algorithms are divided into two categories: Centralized Federated Learning (CFL) and Decentralized Federated Learning (DFL). In a CFL system, all the clients train a model in parallel using their local datasets. Then, the clients send the trained parameters to the server. The server aggregates model parameters after receiving from all clients, and builds the updated global model. The clients get the updated model parameters from the server for the next training round. After the server finishes the global model training, each of the clients has same global model as well as its personalized local model. However, the communication with the server may not be always available. In such a case, DFL can be adopted. In DFL, all the clients form a collaborative network. For each of the communication rounds, the clients use their local datasets for local training. After that, each client performs model aggregation based on model updates received from the neighbour nodes.

### 1.1. Motivation and Contributions

Crop yield prediction is an important domain of smart agriculture, where ML is used for data analysis (Van Klompenburg et al. ((2020))). As farmers' information as well as soil and environmental parameters' data analysis take place, privacy is a major issue. In such a case, the use of conventional cloud-only framework for data analysis using ML raises concern regarding data privacy, latency, connectivity interruption due to poor network connectivity inside the agricultural lands, etc. To address these issues, the objective of the paper is to explore the use of FL for crop yield prediction. The major contributions of the paper are:

- The use of FL in farming practices is discussed, and then an experimental case study is performed to analyse the performance of CFL and DFL in crop yield prediction. We consider a scenario where different number of devices perform collaborative training using CFL and DFL. Long Short-Term Memory (LSTM) Network is used as the underlying approach for both the CFL and DFL mechanisms.
- To implement CFL, a client-server paradigm is developed using socket programming, and multiple clients are handled by the server in the conducted experiment. For transmission of model updates *MLSocket* is used. For aggregation, Federated Averaging (FedAvg) is used. The performance of CFL-based framework has been evaluated in terms of prediction accuracy, precision, recall, F1-Score, and training time. The experimental results present that the CFL-based framework has better prediction accuracy and lower response time than the cloud-only framework where the cloud server analyses the data after receiving from the client.
- To implement the DFL, a collaborative network is formed using mesh topology or ring topology. In the conducted experiment, each node receives model updates from the neighbour nodes (the neighbour nodes depend on the selected topology), and performs aggregation to build the upgraded model. The performance of the nodes in both the

Table 1: Acronyms with full forms

Acronyms	Full form
ANN	Artificial Neural Network
ML	Machine Learning
DL	Deep Learning
FL	Federated learning
CFL	Centralized Federated Learning
DFL	Decentralized Federated Learning
IoT	Internet of Things
IoAT	Internet of Agricultural Things
LSTM	Long Short-Term Memory Network
Bi-LSTM	Bidirectional Long Short-Term Memory Network
FedAvg	Federated Averaging
KNN	K-Nearest Neighbours
DT	Decision Tree
RF	Random Forest
XGBoost	Extreme Gradient Boosting
SVM	Support Vector Machine
MLP	MultiLayer Perceptron
LGBM	Light Gradient Boosting Machine
GRU	Gated Recurrent Unit
MLR	Multiple Linear Regression
NB	Naive Bayes
DNN	Deep Neural Network
RNN	Recurrent Neural Network
P2P	Peer-to-Peer
FTL	Federated Transfer Learning

topology are evaluated in terms of prediction accuracy, precision, recall, F1-Score, and training time.

- Finally, the research challenges with CFL and DFL-based frameworks in crop yield prediction are highlighted in this paper.

### 1.2. Layout of The Paper

The rest of the paper is organized as follows: Section 2 briefly discusses the existing literature on FL, smart agriculture, and crop yield prediction. Section 3 illustrates the use of CFL and DFL in crop yield prediction. An experimental case study is presented in Section 4 on the use of CFL and DFL in crop yield prediction. Section 5 explores the future research directions of FL in crop yield prediction. Finally, Section 6 concludes the paper.

The list of acronyms used in this paper are listed in Table 1.

## 2. Related Work

Crop yield prediction and recommendation is a crucial area of IoT-based smart farming practices (Debauche et al. ((2021)), Boursianis et al. ((2022))). There are several research works carried out on the use of ML and DL in crop yield prediction. In (Thilakarathne et al. ((2022))), the authors explored the use of several ML algorithms such as KNN, DT, RF, XGBoost, and SVM, for crop yield prediction. In (Bakthavatchalam et al. ((2022))), the authors used MLP neural network, decision table, and JRip for crop yield prediction. In (Cruz et al. ((2022))), KNN was used for crop yield prediction. In (Kathiria et al. ((2023))), the authors used several ML approaches such as DT, SVM, KNN, LGBM and RF for crop yield prediction. LSTM, Bi-LSTM, and GRU-based framework were used in (Gopi and Karthikeyan ((2024))) for data analysis to predict crop yield. For crop yield prediction, MLR with ANN was used in (Gopal and Bhargavi ((2019))). In (Dey et al. ((2024))), Bi-LSTM was used for data analysis, and for better network connectivity the use of small cell with computation ability was explored. However, none of the existing approaches adopted FL in their frameworks. The major disadvantage of the conventional ML-based framework is compromise with data privacy as data sharing takes place with the cloud for analysis, requirement of high network bandwidth that may not be available at rural regions, high response time, high network traffic, huge overhead on the cloud server, etc. To address all these issues, FL can be adopted in crop yield prediction.

The concept of FL relies on local data analysis, collaborative training, and generating global as well as personalized models. As no individual dataset is shared and a distributed learning is performed, data privacy is protected (Nguyen et al. ((2021))). Further, due to distributed nature, can be adopted in various IoT applications including healthcare, agriculture, transportation system, etc. The use of FL in IoT was elaborated in (Nguyen et al. ((2021))). The use of FL in fog computing environment was explored in (Zhu et al. ((2024))). In (Atitallah et al. ((2023))), for distributed data analytics FL and transfer learning were adopted to propose an intelligent microservices-based framework for IoT applications. The use of FL in agriculture was explored in a few research works. In (Bera et al. ((2024))), CFL was used for soil health monitoring for irrigation decision making. The authors used CFL based on LSTM and DNN in their work. In (Manoj et al. ((2022))), FL was used for soybean yield prediction using deep residual network-based regression models for risk management in agricultural production. In (Friha et al. ((2022))), FL was used for intrusion detection in IoT-based agricultural systems. For yield forecasting FL was used in (Li et al. ((2024))). For efficient data sharing in agri-food sector, the use of FL was discussed in (Durrant et al. ((2022))). For crop classification, FL was used by (Idoje et al. ((2023))). The authors adopted CFL for crop classification based on Gaussian NB in (Idoje et al. ((2023))). As we observe, the use of FL in crop yield prediction was explored in a few existing works, and most of them focused on the use of CFL. In this paper, we provide an experimental study of both the CFL and DFL in crop yield prediction based on LSTM.

In Table 2, the existing works have been compared with respect to the proposed FL-based framework for crop yield prediction. As we observe from the table, most of the existing works rely on conventional ML/DL-based framework, and compared to the existing

CFL-based framework, this work explores the use of both CFL and DFL (with mesh as well as ring-based networks) in crop yield prediction, and determines the training time as well as response time.

### 3. Federated Learning in Crop Yield Prediction

In Section 1, we have briefly discussed on CFL and DFL. For crop yield prediction both the approaches can be used. In an IoT-based crop yield prediction framework, the IoT devices collect data of soil and environmental parameters such as temperature, humidity, rainfall, soil pH, Nitrogen, Phosphorous, Potassium level, etc. The collected IoT data is processed inside the cloud servers. However, for data privacy protection, to reduce latency and deal with poor network connectivity inside the rural regions containing the agricultural lands, FL is adopted in IoAT. The integration of FL with IoT-based crop yield prediction framework permits the local data analysis inside the edge devices that can work as the clients. For data analysis we have used LSTM in this work. To capture the temporal dependencies and retain the sequential nature of the soil and environmental data, LSTM is considered. The mathematical notations used in this work are defined in Table 3.

LSTM is an upgraded version of RNN that considers a memory cell which is controlled by input gate, forget gate, and output gate. LSTM maintains a chain-like structure that has four neural networks and different memory blocks referred to as cells. To learn long-term dependencies the gates play significant roles by retaining or discarding information in a selective manner. For the short-term memory a hidden state is maintained by the LSTM network, that is updated depending on the previous hidden state, input, and the current state of the memory cell.

In LSTM, the forget gate controls which information will be removed from the memory cell, and mathematically expressed as:

$$\phi_t = \sigma(\text{weight}_\phi \dots [h_{t-1}, x_t] + \text{bias}_\phi) \quad (1)$$

where  $\sigma$  denotes the sigmoid function.

The input gate is used to add information to the memory cell, and mathematically expressed as:

$$\zeta_t = \sigma(\text{weight}_\zeta \dots [h_{t-1}, x_t] + \text{bias}_\zeta) \quad (2)$$

where, a sigmoid function is used to regulate the information and filter the values to retain. After that,  $\tanh$  function is used to create a vector having all possible values from  $h_{t-1}$  and  $x_t$ , as follows:

$$\hat{C}_t = \tanh(\text{weight}_C \dots [h_{t-1}, x_t] + \text{bias}_C) \quad (3)$$

where  $\text{weight}_C$  denotes the weight matrix and  $\text{bias}_C$  denotes the bias.

Finally, the regulated values are multiplied with the values of the vector to get the information to be added to the memory cell, as follows:

$$C_t = \phi_t \odot C_{t-1} + \zeta_t \odot \hat{C}_t \quad (4)$$

Table 2: Comparison of our work with existing crop yield prediction frameworks

Work	Classifier	Multi-crop dataset is used	CFL is used	DFL is used	Training time is measured	Response time is measured
Thilakarathne et al. ((2022))	RF, DT, KNN, XGBoost, SVM	✓	✗	✗	✗	✗
Bakthavatchalam et al. ((2022))	MLP, Decision Table, JRip	✓	✗	✗	Measured model build time	✗
Cruz et al. ((2022))	KNN	✓	✗	✗	✗	✗
Kathiria et al. ((2023))	DT, SVM, KNN, LGBM, RF	✓	✗	✗	✗	✗
Gopi and Karthikeyan ((2024))	LSTM, Bi-LSTM, GRU	✓	✗	✗	✗	✗
Idoje et al. ((2023))	Gaussian NB	✓	✓	✗	✗	✗
Our work	LSTM	✓	✓	✓	✓	✓

Table 3: Mathematical notations with definitions

Notations	Definition
$\phi_t$	Forget gate
$\zeta_t$	Input gate
$\lambda_t$	Output gate
$weight_\phi$	Weight matrix of forget gate
$weight_\zeta$	Weight matrix of input gate
$weight_\lambda$	Weight matrix of output gate
$bias_\phi$	Bias for forget gate
$bias_\zeta$	Bias for input gate
$bias_\lambda$	Bias for output gate
$h_t$	Present hidden state
$h_{t-1}$	Previous hidden state
$x_t$	Current input
$\hat{C}_t$	Candidate value
$C_t$	Cell state
$C_{t-1}$	Previous cell state
$Data_c$	Data of client $c$
$B$	Batch size
$\eta$	Learning rate
$N_b$	Number of batches
$N_e$	Number of epochs
$N_r$	Number of rounds
$m_c$	Model updates of client $c$
$N_c$	Number of connected clients
$f_c$	Fraction of clients participating in CFL
$m_s$	Model parameter of the server
$m_{final}$	Final global model update
$m_0$	Initial model parameters of a node in DFL
$m_p$	Model updates of node $p$ in DFL
$P$	Set of nodes in the DFL framework
$N_p$	Number of neighbours nodes in DFL
$\mathcal{L}$	Loss function
$\alpha$	True positive
$\beta$	True negative
$\gamma$	False positive
$\rho$	False negative
$\mathcal{A}$	Accuracy
$\mathcal{P}$	Precision
$\mathcal{R}$	Recall
$\mathcal{F}$	F1-Score



The output gate that extracts the useful information from the current memory cell state as the output, is mathematically expressed as follows:

$$\lambda_t = \sigma(\text{weight}_\lambda \dots [h_{t-1}, x_t] + \text{bias}_\lambda) \quad (5)$$

Firstly, using *tanh* function a vector is generated. After that, a sigmoid function is used to regulate the information and filter the values to retain using the inputs  $h_{t-1}$  and  $x_t$ . Finally, the regulated values are multiplied with the values of the vector to be sent as an output as well as input to the next cell. As LSTM is able to capture long-term dependencies, LSTM performs well in sequence prediction tasks, time series, etc.

### 3.1. CFL-based framework

In our CFL-based system, all the clients get the initial model parameters from the server, train their individual models using their local datasets, and then transmit the model updates to the server node. The server node works as the aggregator that receives model updates from all the clients and performs aggregation to update the global model accordingly. Here, for aggregation, we use FedAvg. The updated global model is sent to the participating clients. Hence, at the end of the process each client has its personalized local model and the global model. The client and server-side algorithms are stated in Algorithm 1 and Algorithm 2 respectively. In the algorithms,  $c$  represents a client and  $S$  represents the server. Algorithm 1 presents the steps of the client-side process, where each connected client gets model parameters from the server, trains the local model using its local dataset, and returns the model updates to the server. Algorithm 2 presents the steps of the server-side process, where the server receives model updates from the connected clients, performs aggregation, and updates the model accordingly. The pictorial representation of CFL is presented in Fig. 1, where  $N_c$  clients participate in a collaborative training process with the server that works as the aggregator to aggregate the model updates received from the clients to build the global model.

In CFL, the server is the aggregator and it distributes the model updates with the clients. The clients have their personalized models along with the global model update. Each of the clients can perform data analysis locally through a collaborative training process without sharing data. Hence, privacy is protected as well as through collaborative training prediction accuracy is enhanced. The time complexity of the CFL process depends on the time complexity of model initialization, local model training, exchange of model updates, and aggregation. The time complexity of model initialization is given as  $O(1)$ . The time complexity of local model training is given as  $O(N_r \cdot N_e \cdot N_b \cdot m_c)$ . The time complexity of exchanging model updates is given as  $O(N_r \cdot N_c \cdot (m_c + m_s))$ . The time complexity of aggregation is given as  $O(N_r \cdot N_c \cdot m_c)$ .

Though, there are several benefits, the CFL has some limitations. As the server performs as the aggregator, good network connectivity with the server is highly desirable. However, many applications do not have the provision of seamless network connectivity. Further, the overhead on the server is very high because the aggregation takes place inside the server. Further, sharing model updates by all the clients with the server may raise a concern regarding security. To address these limitations, DFL has come.

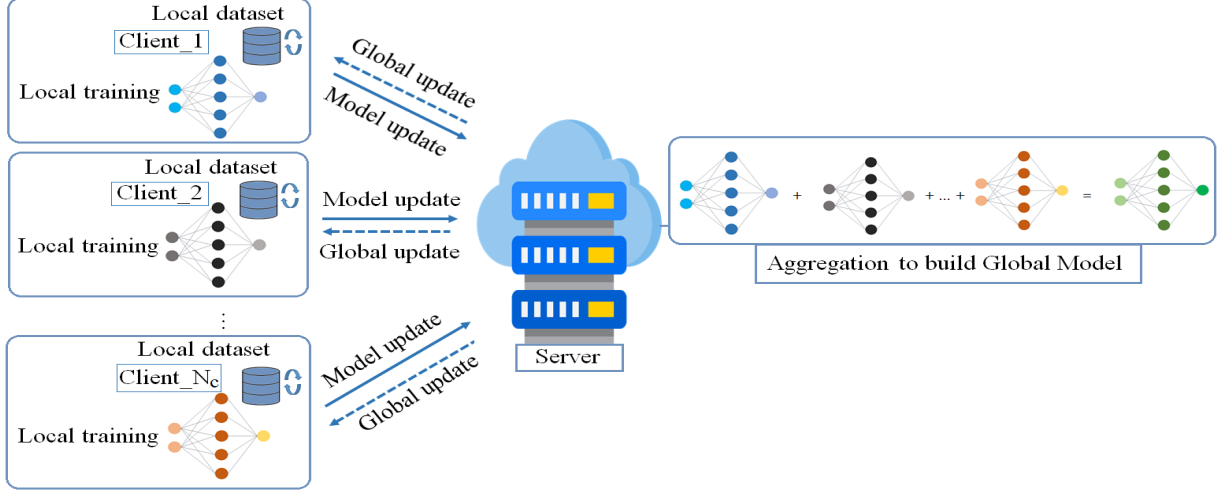


Figure 1: The CFL process

---

**Algorithm 1** Client-side algorithm

---

**Input:**  $Data_c, N_b, N_e$

**Output:**  $m_c$

1: *Function*  $Update(Data_c, N_b, N_e)$ :

2:  $PData_c \leftarrow Preprocess(Data_c)$

3: **while** *connected with*  $S$  **do**

4:      $Train(m_c \leftarrow getmodelparameters())$

5: **end while**

6:  $SaveParameters(m_c)$

7: *Function*  $Train(m_c)$ :

8:  $N_b \leftarrow Split(PData_c, B)$

▷ split data into  $N_b$  batches

9: **for**  $e = 0$  to  $N_e - 1$  **do**

10:     **for**  $b = 1$  to  $N_b$  **do**

11:          $m_c^{e+1} \leftarrow m_c^e - \eta \nabla m_c^e$

▷  $\nabla m_c^e$  represents the gradient

12:     **end for**

13: **end for**

14:  $m_c \leftarrow m_c^{N_e}$

15:  $sendmodelupdate(m_c)$

▷ send model update to  $S$

---

---

**Algorithm 2** Server-side Algorithm

---

**Input:**  $N_c, f_c, N_r$

**Output:**  $m_{final}$

```
1: Function Collect( $N_c, N_r$ ):
2: ConnectedClients  $\leftarrow \square$ 
3: while (length(ConnectedClients)  $\neq N_c$ ) do
4:   listen()
5:   acceptconnection()
6: end while
7: FedAvg()
8: Release clients
9: Function FedAvg():
10:  $m_s^0 \leftarrow \text{InitModel}()$  ▷ initial model is generated
11: for  $r = 1$  to  $N_r$  do
12:    $M_r \leftarrow \text{Subset}(\max(f_c * N_c, 1), \text{"random"})$ 
13:    $MU \leftarrow \square$ 
14:   for  $c \in M_r$  do
15:      $m_c^r \leftarrow \text{getmodelupdate}(c)$  ▷ get model update from client  $c$  at round  $r$ 
16:      $MU.append(m_c^r)$ 
17:   end for
18:    $m_s^{r+1} \leftarrow \frac{1}{N_c} \sum_{c=1}^{N_c} m_c^r$ 
19:   sendtoclients( $m_s^{r+1}$ )
20: end for
21:  $m_{final} \leftarrow m_s^{N_r+1}$ 
```

---

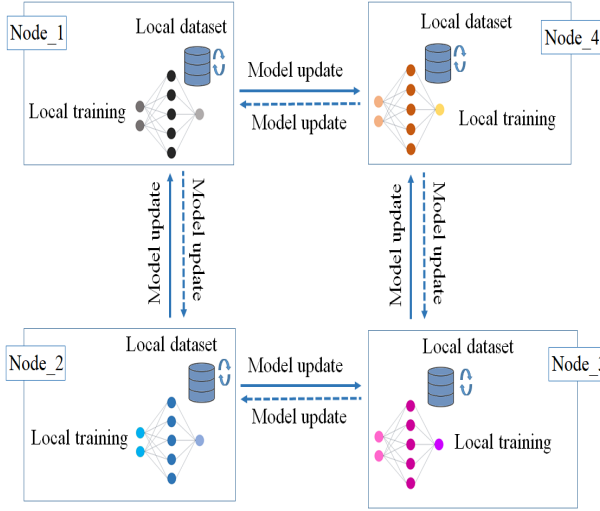


Figure 2: DFL using ring-based network

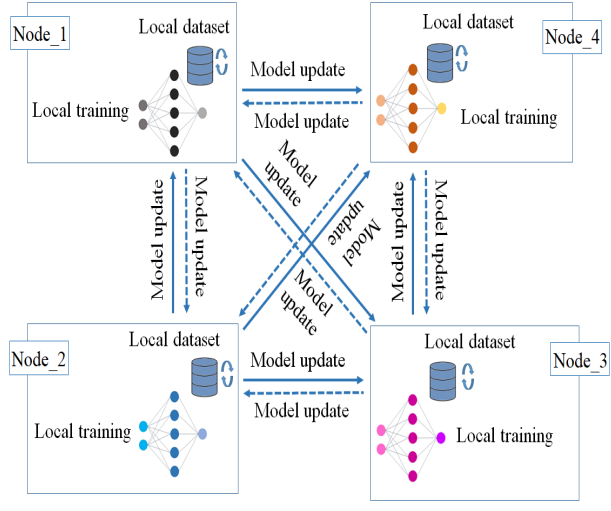


Figure 3: DFL using mesh-based network

### 3.2. DFL-based framework

In case of crop yield prediction, the data collection takes place at the rural regions, where the network connectivity is usually poor. In that case, the communication with the cloud server is a major issue. Therefore, if the network connectivity is poor, DFL can be used by the edge devices for collaborative training purpose. In DFL, the clients form a network among themselves and perform collaborative learning. Here, each node is a learner as well as contributor. In our work, we have considered two types of DFL frameworks where the clients form a network either using ring or mesh topology. The ring-based network is referred to as P2P network also, where each peer exchanges its model updates with two neighbour nodes. In case of the mesh-based network, each node exchanges its model updates with rest of the nodes in that network. The DFL process for ring-based and mesh-based networks are stated in Algorithm 3 and Algorithm 4 respectively, where  $p$  denotes a node and  $P$  denotes the set of nodes in the formed network. The pictorial representation of DFL using ring-based and mesh-based networks are presented in Figs. 2 and 3, where four nodes form a network using ring topology and mesh topology respectively.

We observe from Algorithm 3 that in the ring-based DFL approach, a node  $p$  sends and receives model updates to and from its preceding node ( $p_{pre}$ ) and the succeeding node ( $p_{suc}$ ). In the mesh-based DFL approach as presented in Algorithm 4, a node  $p$  sends and receives model updates to and from rest of the nodes of the network. In Algorithms 3 and 4, we have initially considered an empty array  $M_{recv}$ . As the model updates are received from the neighbour nodes, the received updates are appended to store all the received updates inside  $M_{recv}$ . Finally, aggregation takes place based on the received updates from the nodes in both the ring-based and mesh-based networks. The time complexity of the DFL-based framework depends on the time complexity of model initialization, local model training, exchanging model updates, and aggregation. The time complexity of model initialization is given as  $O(1)$ . The time complexity of local model training is given as  $O(N_r \cdot N_e \cdot N_b \cdot m_p)$ .

---

**Algorithm 3** Model update in Ring-based P2P Network

---

**Input:**  $P, N_p, m_0, N_r$ **Output:**  $m_p, \forall p \in P$ 

```
1: Function Training( $N_p, m_0$ ):
2: for  $p = 1$  to  $|P|$  do
3:    $m_p \leftarrow m_0$  ▷ Initialize model parameters
4: end for
5: for  $r = 1$  to  $N_r$  do
6:   for  $p = 1$  to  $|P|$  do ▷ Local model training
7:      $PData_p \leftarrow Preprocess(Data_p)$ 
8:      $N_b \leftarrow Split(PData_p, B)$  ▷ split data into  $N_b$  batches
9:     for  $e = 0$  to  $N_e - 1$  do
10:      for  $b = 1$  to  $N_b$  do
11:         $m_p^{e+1} \leftarrow m_p^e - \eta \nabla m_p^e$  ▷  $\nabla m_p^e$  represents the gradient
12:      end for
13:    end for
14:  end for
15:  for  $p = 1$  to  $|P|$  do ▷ Exchange of model updates and aggregation
16:     $M_{recv} \leftarrow []$ 
17:    Send  $m_p$  to  $p_{pre}$  and  $p_{suc}$ 
18:     $m_j^r \leftarrow getmodelupdate(j)$ , where  $j \in \{p_{pre}, p_{suc}\}$ 
19:     $M_{recv}.append(m_j^r)$ 
20:     $m_p^{r+1} \leftarrow \sum_{j=1}^{N_p} m_j^r / N_p$  ▷ Aggregate model updates received from  $p_{pre}$  and  $p_{suc}$ 
21:  end for
22: end for
```

---

---

**Algorithm 4** Model update in Mesh-based Network

---

**Input:**  $Data_p, P, N_p, m_0, N_r$ **Output:**  $m_p, \forall p \in P$ 

```
1: Function Training( $N_p, m_0$ ):
2: for  $p = 1$  to  $|P|$  do
3:    $m_p \leftarrow m_0$  ▷ Initialize model parameters
4: end for
5: for  $r = 1$  to  $N_r$  do
6:   for  $p = 1$  to  $|P|$  do ▷ Local model training
7:      $PData_p \leftarrow Preprocess(Data_p)$ 
8:      $N_b \leftarrow Split(PData_p, B)$  ▷ split data into  $N_b$  batches
9:     for  $e = 0$  to  $N_e - 1$  do
10:      for  $b = 1$  to  $N_b$  do
11:         $m_p^{e+1} \leftarrow m_p^e - \eta \nabla m_p^e$  ▷  $\nabla m_p^e$  represents the gradient
12:      end for
13:    end for
14:  end for
15:  for  $p = 1$  to  $|P|$  do ▷ Exchange of model updates and aggregation
16:     $M_{recv} \leftarrow []$ 
17:    for  $j = 1$  to  $N_p$  do
18:      Send  $m_p$  to  $j$ , where  $j \in (P - p)$ 
19:       $m_j^r \leftarrow getmodelupdate(j)$ , where  $j \in (P - p)$ 
20:       $M_{recv}.append(m_j^r)$ 
21:    end for
22:     $m_p^{r+1} \leftarrow \sum_{j=1}^{N_p} m_j^r / N_p$  ▷ Aggregate model updates received from all other nodes
23:  end for
24: end for
```

---

The time complexity of exchanging model updates is given as  $O(N_r \cdot N_p \cdot (m_p + m_j))$ . The time complexity of aggregation is given as  $O(N_r \cdot N_p \cdot m_j)$ , where  $1 \leq j \leq N_p$ .

If a DFL framework contains three nodes, then the number of exchange of model updates will be same for both the mesh and ring-based networks. However, for the *number of nodes*  $>= 4$ , the results will be different as the number of model updates exchange differ for the mesh and ring-based networks.

### 3.3. Proof of Convergence in FL

For both the CFL and DFL approaches, the final objective is to minimize the global loss function  $\mathcal{L}(m)$  that is mathematically defined as follows:

$$\mathcal{L}(m) = \frac{1}{K} \sum_{i=1}^K \mathcal{L}_i(m) \quad (6)$$

where  $K$  is the number of participating nodes, i.e.  $K = N_c$  for CFL and  $K = N_p$  for DFL, and  $\mathcal{L}_i(m)$  is the local loss function at node  $i$ .

**Definition IV.1.** *Lipschitz Continuity:*  $\mathcal{L}_i(m)$  is  $\mathcal{L}$ -Lipschitz continuous if there exists a constant  $C_1 > 0$  such that  $\forall m, \mathbf{w}$ , we have

$$\mathcal{L}_i(m) \leq \mathcal{L}_p(\mathbf{w}) + \nabla \mathcal{L}_p(\mathbf{w})^T (m - \mathbf{w}) + \frac{C_1}{2} \|m - \mathbf{w}\|^2 \quad (7)$$

**Definition IV.1.** *Bounded Variance:* The variance of the stochastic gradients is bounded if there exists a constant  $C_2^2 > 0$  such that  $\forall m$ :

$$\mathbb{E}[\|\nabla \mathcal{L}_i(m) - \nabla \mathcal{L}(m)\|^2] \leq C_2^2 \quad (8)$$

**Definition IV.1.** *Unbiased Gradients:* The stochastic gradients are unbiased estimates of the true gradients if  $\forall m$ :

$$\mathbb{E}[\nabla \mathcal{L}_i(m)] = \nabla \mathcal{L}(m) \quad (9)$$

**Assumption IV.1.** *Smoothness:* The global loss function  $\mathcal{L}(m)$  is smooth, i.e., there exists a constant  $C_3 > 0$ , such that  $\forall m, \mathbf{w}$ :

$$\mathcal{L}(m) \leq \mathcal{L}(\mathbf{w}) + \nabla \mathcal{L}(\mathbf{w})^T (m - \mathbf{w}) + \frac{C_3}{2} \|m - \mathbf{w}\|^2 \quad (10)$$

**Assumption IV.2.** *Strong Convexity:* The global loss function  $\mathcal{L}(m)$  is strongly convex, i.e., there exists a constant  $C_4 > 0$  such that  $\forall m, \mathbf{w}$ :

$$\mathcal{L}(m) \geq \mathcal{L}(\mathbf{w}) + \nabla \mathcal{L}(\mathbf{w})^T (m - \mathbf{w}) + \frac{C_4}{2} \|m - \mathbf{w}\|^2 \quad (11)$$

**Lemma IV.1.** *Gradient Bound: Under the assumptions of Lipschitz continuity and bounded variance, the gradient of  $\mathcal{L}(m)$  is bounded:*

$$\mathbb{E}[\|\nabla\mathcal{L}(m)\|^2] \leq \frac{C_1}{K} \sum_{i=1}^K \|\nabla\mathcal{L}_i(m)\|^2 + \frac{C_2^2}{K} \quad (12)$$

*Proof.* By Lipschitz continuity of  $\mathcal{L}_i(m)$ :

$$\|\nabla\mathcal{L}_i(m)\|^2 \leq C_1^2 \|m\|^2 \quad (13)$$

Taking the expectation and summing over all nodes:

$$\mathbb{E}[\|\nabla\mathcal{L}(m)\|^2] = \frac{1}{K^2} \sum_{i=1}^K \mathbb{E}[\|\nabla\mathcal{L}_i(m)\|^2] \leq \frac{C_1^2}{K^2} \sum_{i=1}^K \|m\|^2 + \frac{C_2^2}{K} \quad (14)$$

Thus,

$$\mathbb{E}[\|\nabla\mathcal{L}(m)\|^2] \leq \frac{C_1}{K} \sum_{i=1}^K \|\nabla\mathcal{L}_i(m)\|^2 + \frac{C_2^2}{K} \quad (15)$$

□

**Theorem IV.1.** *Under the Lipschitz continuity, bounded variance, unbiased gradients, smoothness, and strong convexity, the FL-based framework converges to a stationary point of  $\mathcal{L}(m)$ .*

*Proof. Step 1: Local Update Rule:* Each node  $i$  performs local updates using stochastic gradient descent for  $N_e$  local epochs. Let  $m_i^e$  denotes the model parameters at node  $i$  at epoch  $e$ , then

$$m_i^{e+1} = m_i^e - \eta \nabla m_i^e \quad (16)$$

*Step 2: Aggregation:* After  $N_e$  epochs, each node exchanges its model updates with other nodes in DFL, and with the server in CFL. For CFL, the aggregation takes place at the server. After receiving the model update, the client trains with local dataset, and sends the updates to the server.

For CFL, the global model update at round  $r$  is defined as:

$$m^{r+1} = \frac{1}{K} \sum_{i=1}^K m_i^r \quad (17)$$

where  $K = N_e$ .

For DFL, each node aggregates the updates after receiving from neighbour nodes ( $N_p$ ). Hence, the local model update at round  $r$  is defined as:

$$m_i^{r+1} = \frac{1}{N_p} \sum_{j=1}^{N_p} m_j^r \quad (18)$$



The global model update at round  $r$  is defined as:

$$m^{r+1} = \frac{1}{K} \sum_{i=1}^K m_i^{r+1} \quad (19)$$

where  $K = N_p$ .

*Step 3: Bounding the Global Loss:* Using the smoothness assumption, the change in  $\mathcal{L}(m)$  is expressed as follows:

$$\mathcal{L}(m^{r+1}) \leq \mathcal{L}(m^r) + \nabla \mathcal{L}(m^r)^{N_r} (m^{r+1} - m^r) + \frac{C_2}{2} \|m^{r+1} - m^r\|^2 \quad (20)$$

Taking the expectation over the stochastic gradients, we obtain

$$\mathbb{E}[\mathcal{L}(m^{r+1})] \leq \mathcal{L}(m^r) - \frac{\eta}{K} \|\nabla \mathcal{L}(m^r)\|^2 + \frac{C_3 \eta^2 C_2^2}{2K} \quad (21)$$

Now, summing this inequality over  $N_r$  rounds, we get

$$\sum_{r=1}^{N_r} \mathbb{E}[\mathcal{L}(m^{r+1}) - \mathcal{L}(m^r)] \leq -\frac{\eta}{K} \sum_{r=1}^{N_r} \|\nabla \mathcal{L}(m^r)\|^2 + \frac{C_3 \eta^2 C_2^2 N_r}{2K} \quad (22)$$

After rearranging terms, we find

$$\frac{1}{N_r} \sum_{r=1}^{N_r} \mathbb{E}[\|\nabla \mathcal{L}(m^r)\|^2] \leq \frac{\mathcal{L}(m^1) - \mathcal{L}(m^{N_r+1})}{\eta N_r} + \frac{C_3 \eta C_2^2}{2K} \quad (23)$$

As  $N_r \rightarrow \infty$ , the term  $\frac{\mathcal{L}(m^1) - \mathcal{L}(m^{N_r+1})}{\eta N_r}$  approaches zero, ensuring the following

$$\lim_{N_r \rightarrow \infty} \frac{1}{N_r} \sum_{r=1}^{N_r} \mathbb{E}[\|\nabla \mathcal{L}(m^r)\|^2] = 0 \quad (24)$$

This demonstrates that the global model updates  $m$  converge to a stationary point of  $\mathcal{L}(m)$ .  $\square$

### 3.4. Performance metrics

In the next section, we have analysed the performance of both the CFL and DFL-based frameworks in crop yield prediction in terms of prediction accuracy, precision, recall, F1-Score, and training time.

The accuracy of a model is determined as follows:

$$\mathcal{A} = \frac{\alpha + \beta}{\alpha + \beta + \gamma + \rho} \quad (25)$$

The precision of a model is determined as follows:

$$\mathcal{P} = \frac{\alpha}{\alpha + \gamma} \quad (26)$$

The recall of a model is determined as follows:

$$\mathcal{R} = \frac{\alpha}{\alpha + \rho} \quad (27)$$

The F1-Score of a model is determined as follows:

$$\mathcal{F} = 2 * \frac{\mathcal{P} * \mathcal{R}}{\mathcal{P} + \mathcal{R}} \quad (28)$$

We have already discussed the time complexity of CFL and DFL, where we observe that the time consumption depends on the time consumed for model initialization, training, exchange of model updates, and aggregation.

Therefore, in the CFL-based approach, the training time of the server is determined as the sum of the time consumption for model initialization ( $T_{init_1}$ ), model training ( $T_{train_1}$ ), exchanging updates with the clients ( $T_{ex_1}$ ), and aggregation ( $T_{agg_1}$ ), given as,

$$T_{CFL} = T_{init_1} + T_{train_1} + T_{ex_1} + T_{agg_1} \quad (29)$$

In the DFL-based framework, the training time of a node is determined as the sum of the time consumption for model initialization ( $T_{init_2}$ ), model training ( $T_{train_2}$ ), exchanging updates with the neighbour nodes ( $T_{ex_2}$ ), and aggregation ( $T_{agg_2}$ ), given as,

$$T_{DFL} = T_{init_2} + T_{train_2} + T_{ex_2} + T_{agg_2} \quad (30)$$

## 4. Performance Evaluation

This section describes the implementation, experimental setup used for analysis, and then analyses the performance of CFL and DFL based on the experimental setup.

### 4.1. Implementation

A design and implementation of the architecture of CFL shown in Fig. 1 is presented in Fig. 4 along with detailing interaction between FL clients and the global server. In Figs. 2 and 3, we have presented the architecture of DFL using ring and mesh topology respectively. Here, we present the implementation diagrams of DFL using ring and mesh topology with four nodes in Figs. 5 and 6, respectively. For implementation, we use Python language. *Tensorflow* is used along with LSTM supported by it. To build the client-server model and communication over the network, socket programming is used. For the transfer of model updates, we used *MLSocket*. For secure communication, Secure Shell protocol is used. The considered dataset is split, and assigned to the clients as the local datasets, and to the server as the global dataset. As the first and second dense layer activation function *ReLU* is used. *Softmax* is used as the Output layer activation function. *Sparse Categorical Crossentropy* is used as the Loss function, and as the optimizer *Adam* is used.

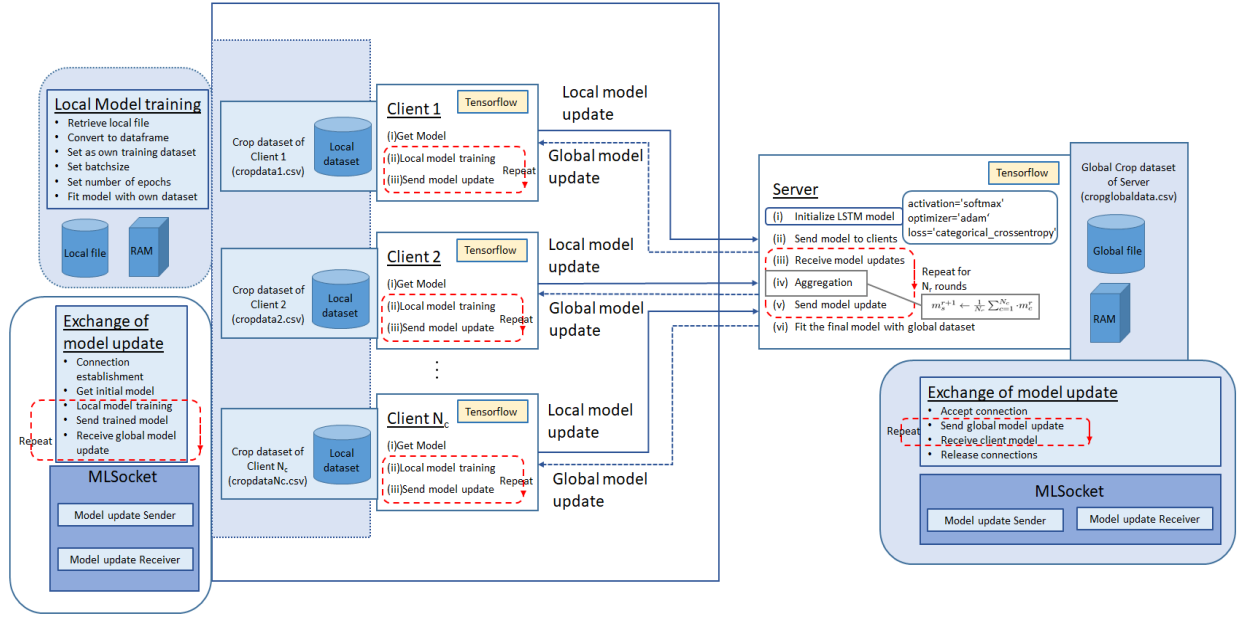


Figure 4: The experimental implementation diagram of CFL-based crop yield prediction

#### 4.2. Experimental setup

The experiment was conducted in the CLOUDS lab, The University of Melbourne. We created *sixteen instances (H1 to H16)* over *RONIN Cloud Platform*. The configuration of each instance is:

- 4GB RAM
- 2 vCPUs
- 100GB SSD

Among these instances *one instance (H3)* was selected as the *server machine*, and other *fifteen instances (H1, H2, H4-H15)* served as the *client machines*. The performance of CFL and DFL in crop yield prediction were analysed in terms of prediction accuracy and training time. For experimental analysis we used the dataset<sup>1</sup>, containing 2200 samples of 22 different classes (rice, maize, pigeonpeas, chickpea, mothbeans, mungbean, kidneybeans, blackgram, lentil, jute, grapes, pomegranate, watermelon, mango, muskmelon, orange, papaya, banana, apple, coconut, cotton, coffee). There are seven features: Nitrogen (N), Phosphorous (P), Potassium (K), temperature, pH, humidity, and rainfall, which were considered as the input, and the crop was considered as the output. The learning rate was considered 0.001. The number of local epochs was considered 100 in both CFL and DFL.

<sup>1</sup><https://www.kaggle.com/datasets/atharvaingle/crop-recommendation-dataset>

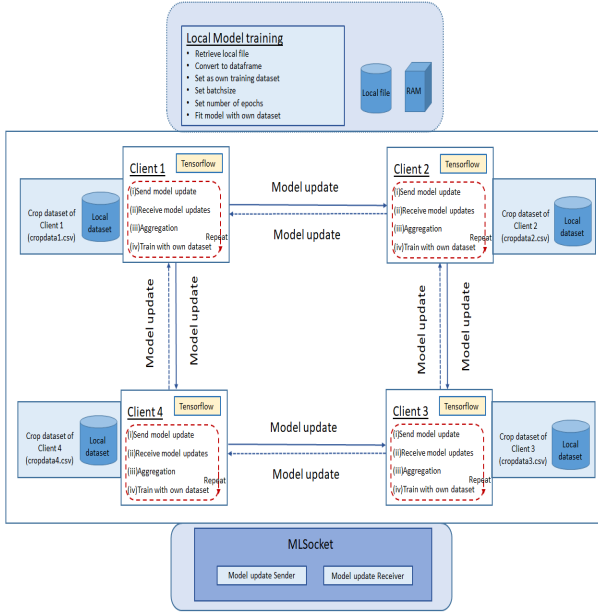


Figure 5: The experimental implementation diagram of DFL-based crop yield prediction using ring topology

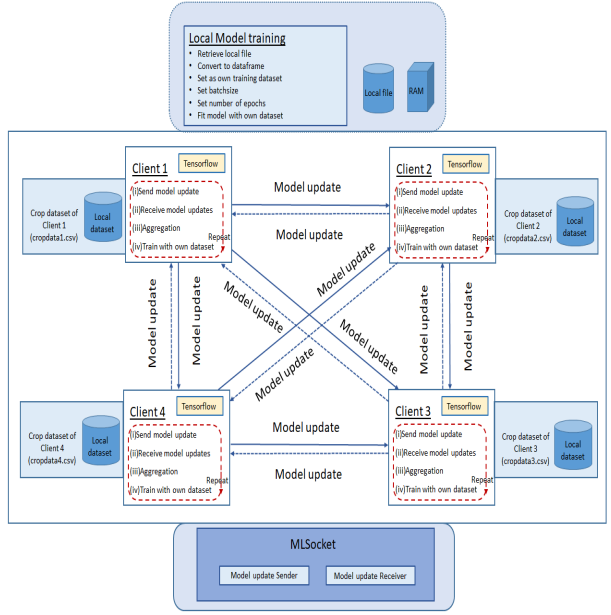


Figure 6: The experimental implementation diagram of DFL-based crop yield prediction using mesh topology

### 4.3. CFL in crop yield prediction

In CFL, we performed three case studies: (i) Scenario 1: Five instances as client machines and one instance as the server machine, (ii) Scenario 2: Ten instances as client machines and one instance as the server machine, and (iii) Scenario 3: Fifteen instances as client machines and one instance as the server machine. Each of the client machines had its local dataset, and the server machine had the global dataset. The client machines shared their model updates with the server machine. The server machine performed aggregation, and updated the global model. The global model update was then shared with the clients. The maximum number of rounds was considered 10. However, we achieved a global model with accuracy of above 0.95 after two rounds, and the difference between the accuracy level for two consecutive rounds was  $< 0.001$  after three rounds.

In *Scenario 1*, five instances (H1, H2, H4, H5, and H6) worked as the client machines and shared their model updates with instance H3 acting as the server machine. The server updated its global model after aggregation, and shared the model update with the five clients. The prediction accuracy of the global model before and after FL are presented in Figs. 7 and 8 respectively. As we observed from the experiment, the global model's accuracy was improved from  $\sim 0.93$  to  $\sim 0.98$  using CFL. The global loss with respect to the number of epochs are presented in Figs. 9 and 10, without using FL and using CFL, respectively. Without using FL, the loss after 100 epochs is  $< 0.5$ , and using CFL, the global loss is  $< 0.0002$  after 100 epochs, as we observe from the figures. In Section 3.3, we have theoretically proved that the global loss tends to 0 as the number of rounds increases. Here, we have presented the result after three rounds, and we observed from the experiment that

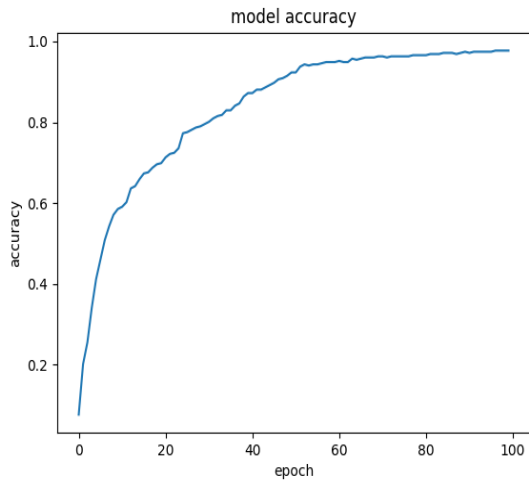


Figure 7: Accuracy of the global model before FL

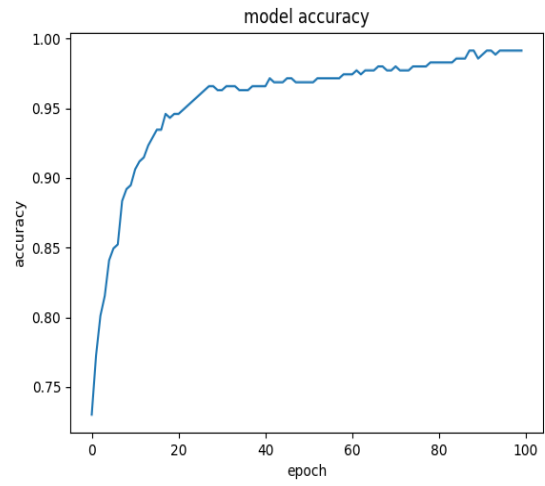


Figure 8: Accuracy of the global model after FL

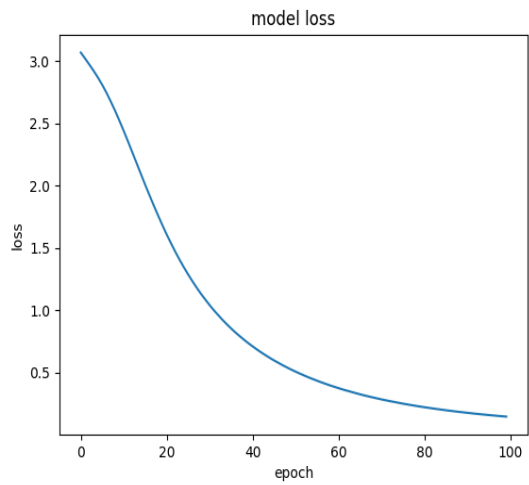


Figure 9: Global loss before FL

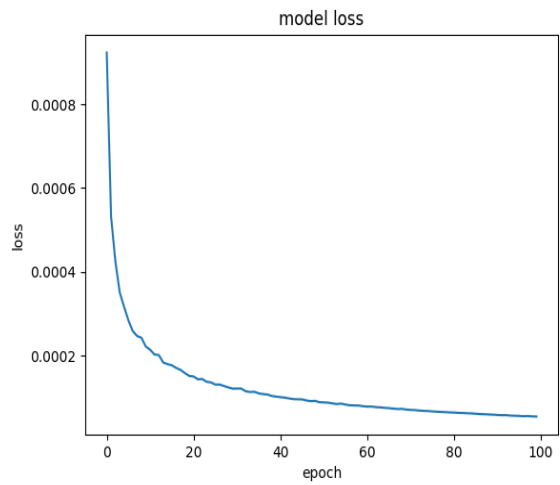


Figure 10: Global loss after using CFL

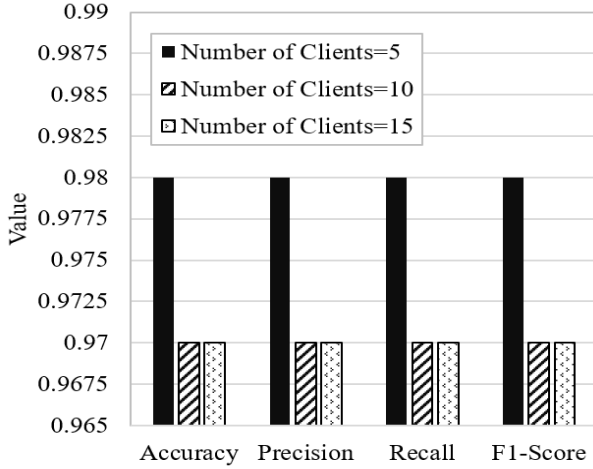


Figure 11: Accuracy, precision, recall, and F1-Score of the global model after FL

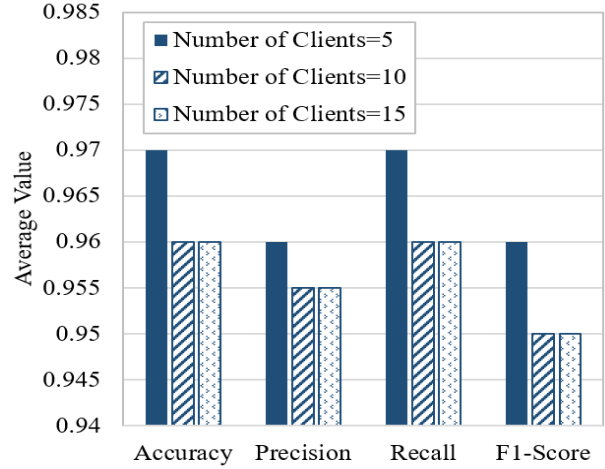


Figure 12: Average accuracy, precision, recall, and F1-Score of the local models after FL

after 10 rounds the loss is below 0.0001, which is almost negligible.

We conducted the experiment for *Scenarios 2 and 3* also. The prediction accuracy we obtained for the global model after CFL in both the scenarios is 0.97. The prediction accuracy, precision, recall, and F1-Score for the three scenarios 1, 2, and 3, are presented in Fig. 11. As we observe, the accuracy, precision, recall, and F1-Score for scenarios 2 and 3 are 0.97, and for scenario 1 all the accuracy metrics provide the value of 0.98. The prediction accuracy, precision, recall, and F1-Score for the clients are presented in Fig. 12. From the experiment we observed that the accuracy, precision, recall, and F1-Score of all the local models after CFL were  $\geq 0.95$ . For the local models, the average accuracy obtained for scenarios 1, 2, and 3 were 0.97, 0.96, and 0.96 respectively. We observe from Figs. 11 and 12 that the accuracy, precision, and recall of the local models and the global model in all three scenarios are above 0.95. Further, the F1-Score of the local models as well as the global model are  $\geq 0.95$  in all three scenarios.

Each of the clients has its own local dataset. Thus, the weights of different local models are different. The server updates the global model after receiving model updates from all the clients. As the model weights of different clients vary, the accuracy of the global model also can differ for different number of clients participating in CFL. However, as we observed from the experiment for all the three scenarios, the accuracy of the global model has been improved than the global model before using CFL. The local models are also updated after receiving the global model update from the server. As the number of clients participating in the CFL varies, the average accuracy may differ for different number of clients. However, we observe that the accuracy of the local models for all three scenarios are above 0.95. Hence, we can recommend the use of FL to achieve a global model with high prediction accuracy and privacy protection without sharing the dataset. The higher accuracy, precision, recall, and F1-Score of global and local models indicate the models provide accurate prediction with stability.

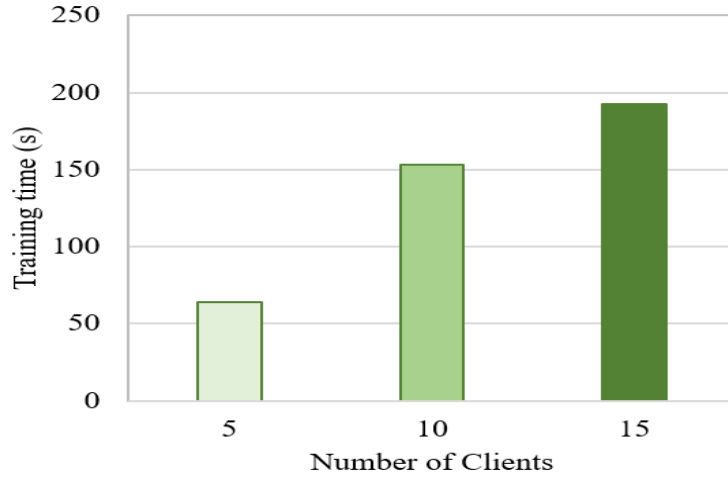


Figure 13: Training time of the global model

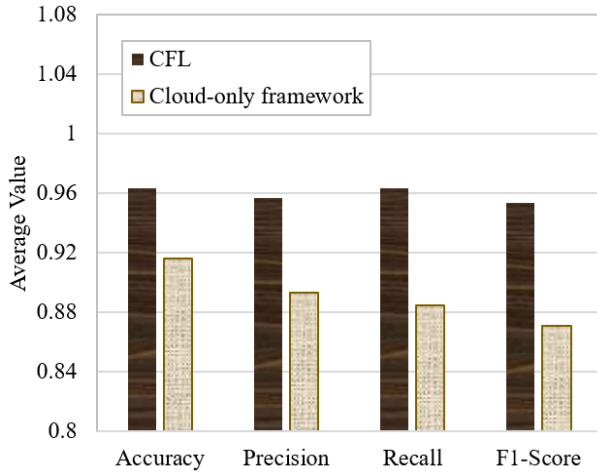


Figure 14: Comparison of average accuracy, precision, recall, and F1-Score between the CFL-based and cloud-only frameworks

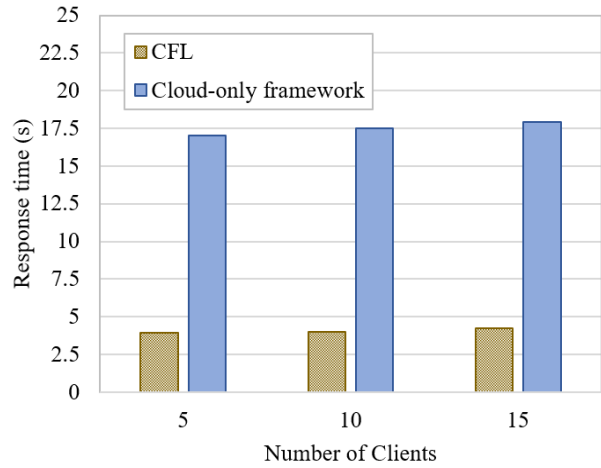


Figure 15: Comparison of response time between the CFL-based and cloud-only frameworks

The training time for the global model for scenarios 1, 2, and 3 are presented in Fig. 13. The training time is measured in seconds (s). As observed from the results, the training time of the global model for scenarios 1, 2, and 3 are 64.13 s, 153.04 s, and 192.33 s respectively. Here, the training time is measured as the sum of the time consumption in model initialization, local model training, exchanging model updates with participating nodes, and aggregation. As the number of clients increase, the delay in receiving updates from the clients increase though parallel communication takes place. As the aggregation takes place only after receiving updates from all the participating clients, the training time increases with the number of participating clients. Thus, the training time for scenario 1 with five clients is low compared to the other two scenarios.

#### 4.3.1. Comparison with Cloud-only framework

The CFL-based framework is compared with the cloud-only framework with respect to accuracy, precision, recall, F1-Score, and response time. By response time, we refer to the difference between the time stamps of submission of request and receiving response from the device regarding crop yield prediction. In this case, again we conducted the experiment for five, ten, and fifteen clients. Each of the clients sent its dataset to the server for analysis. The time consumption in sending the dataset, performing analysis on the dataset using LSTM, sending result to the client, and receiving result by the client, were measured. We observed that the response time for the cloud-only framework was higher than the CFL-based framework. We also observed that the prediction accuracy for the clients' datasets were also lower than the CFL-based framework. In Fig. 14, the average accuracy, precision, recall, and F1-Score of the local models after CFL are compared to the cloud-only framework. Fig. 15 presents the comparison of the response time of the CFL-based model to the cloud-only framework. The CFL-based framework reduces the response time  $\sim 75\%$  than the cloud-only framework. The average accuracy, precision, recall, and F1-Score are also improved by  $\sim 5\%$ ,  $\sim 7\%$ ,  $\sim 8\%$ , and  $\sim 9\%$  using CFL than the cloud-only framework. Hence, we observe that the CFL-based framework outperforms the cloud-only framework.

#### 4.4. DFL in crop yield prediction

The CFL-based framework though has high prediction accuracy, there are several limitations such as increase in overhead on the cloud, security, requirement of high bandwidth, etc. To address these limitations, DFL has been introduced as we have discussed earlier. In DFL, the clients form a collaborative network among themselves. In this work, we used DFL frameworks with ring and mesh topology. Here, also we considered three network scenarios: (i) Four nodes form the network, (ii) Seven nodes form the network, and (iii) Ten nodes form the network. In ring topology, each node exchanges model updates only with the preceding and succeeding nodes. In mesh topology, each node exchanges model updates with rest of the nodes in the formed network. In *Scenario 1*, we had considered four nodes (H1, H2, H4, and H5), which were connected either using ring topology or mesh topology. H3 worked as the server in our experiment. While using ring topology, the prediction accuracy of all the four nodes after DFL are presented in Figs. 16, 17, 18, and 19, respectively. The maximum number of rounds we had considered 10, and the number of local epochs were considered



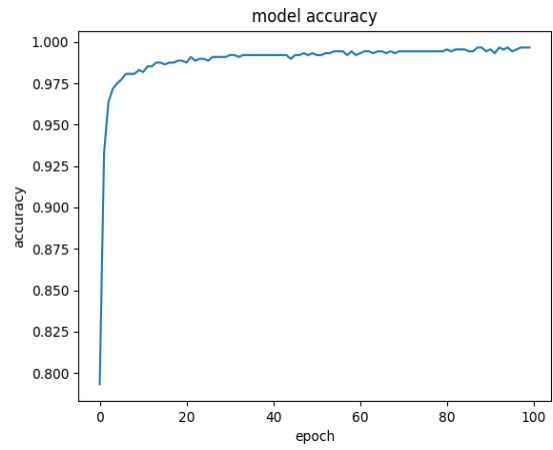
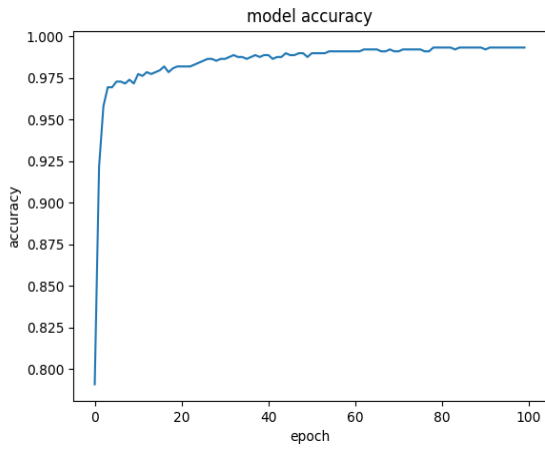


Figure 16: Accuracy of Node1 in ring-based network Figure 17: Accuracy of Node2 in ring-based network

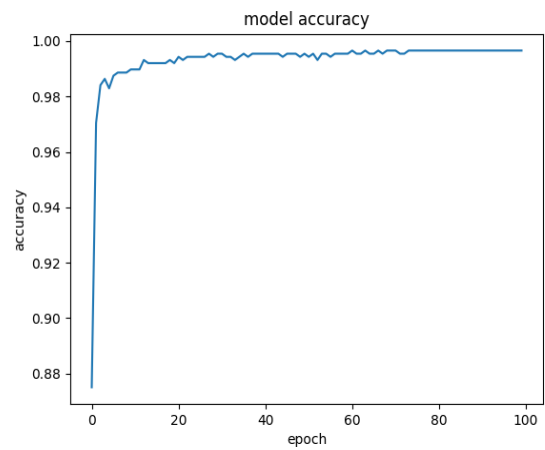
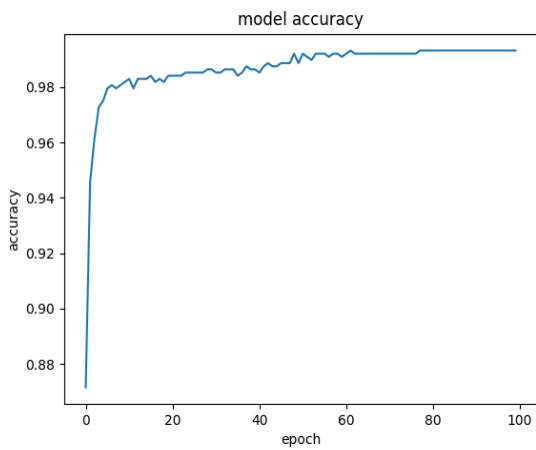


Figure 18: Accuracy of Node3 in ring-based network Figure 19: Accuracy of Node4 in ring-based network

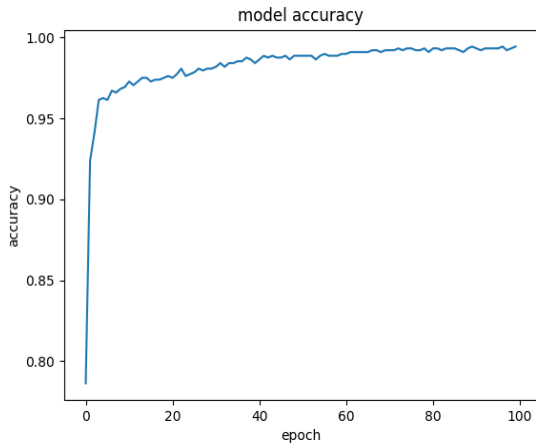


Figure 20: Accuracy of Node1 in mesh-based network

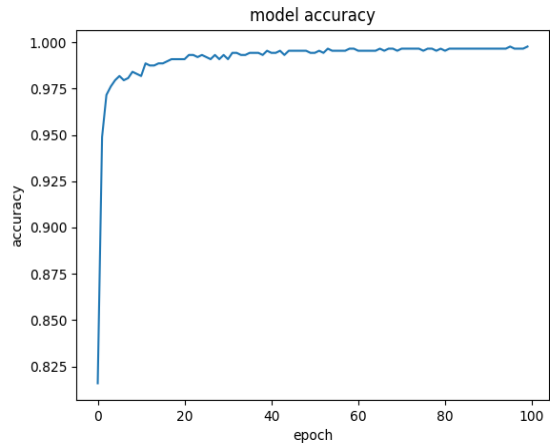


Figure 21: Accuracy of Node2 in mesh-based network

100. In the considered ring-based P2P network, H1 shares its model updates with H2 and H5, H2 shares its model updates with H1 and H4, H4 shares its model updates with H2 and H5, and H5 shares its model updates with H1 and H4. After receiving model updates each of the node performs aggregation and updates their local models accordingly. In the conducted experiment, the prediction accuracy of nodes 1 (H1), 2 (H2), 3 (H4), and 4 (H5) were 0.98, 0.98, 0.98, and 0.99 respectively, while using the ring-based P2P network. As the datasets of the nodes are different, their prediction accuracy may also differ. However, we observed that the prediction accuracy was above 0.97 for all the nodes, and the prediction accuracy of the global model developed by the nodes was 0.98.

The prediction accuracy of all the four nodes while using mesh topology are presented in Figs. 20, 21, 22, and 23, respectively. In the mesh-based network, each node shares its model updates with rest of the nodes. From the results we observe that the prediction accuracy of nodes 1, 2, 3, and 4, after FL were 0.97, 0.97, 0.99, and 0.99 respectively. Here, also the nodes' datasets are different and accuracy level may also therefore vary. However, the accuracy obtained for all the nodes was above 0.96, and the prediction accuracy of the global model developed by the nodes was 0.98.

The accuracy, precision, recall, and F1-Score for the four nodes in ring topology and in mesh topology are presented in Figs. 24 and 25 respectively. We observe from the results that the accuracy, precision, recall, and F1-Score for all the nodes are above 0.96 for both the ring and mesh topology-based networks. Hence, we observe that using DFL high prediction accuracy can be obtained. The training time of the four nodes in ring and mesh-based network are presented in Fig. 26. As we observed in ring-based network the training time of nodes 1, 2, 3 and 4 are 35.53 s, 27.86 s, 31.84 s, and 30.62 s respectively. We also observed that the training time of the nodes 1, 2, 3, and 4 are 36.99 s, 39.65 s, 36.8 s, and 32.97 s, while using the mesh-based network.

The global loss while using DFL using ring and mesh topology, are presented in Figs.

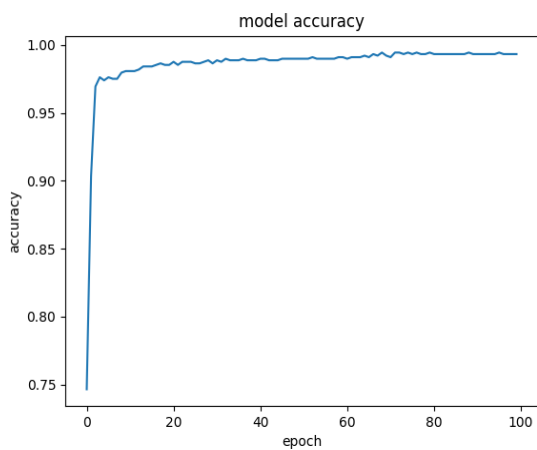


Figure 22: Accuracy of Node3 in mesh-based network

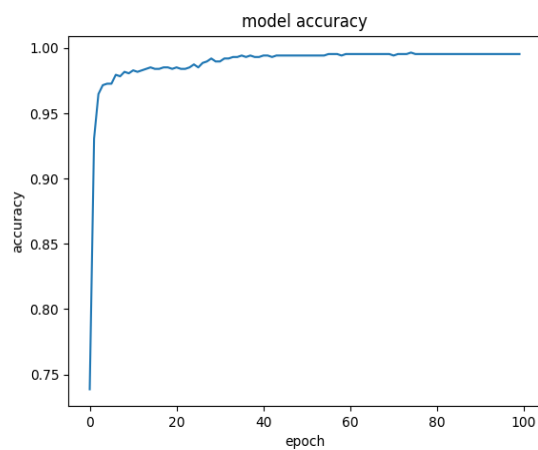


Figure 23: Accuracy of Node4 in mesh-based network

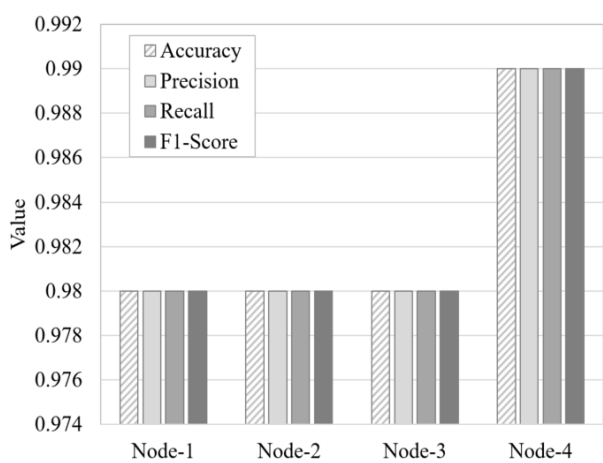


Figure 24: Accuracy, precision, recall, and F1-Score of the local models in ring-based network

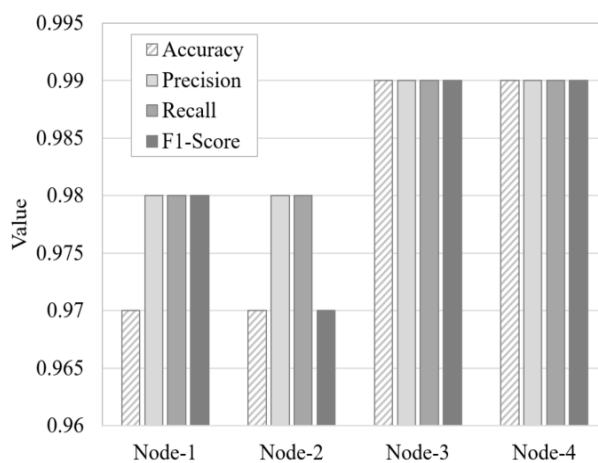


Figure 25: Accuracy, precision, recall, and F1-Score of the local models in mesh-based network

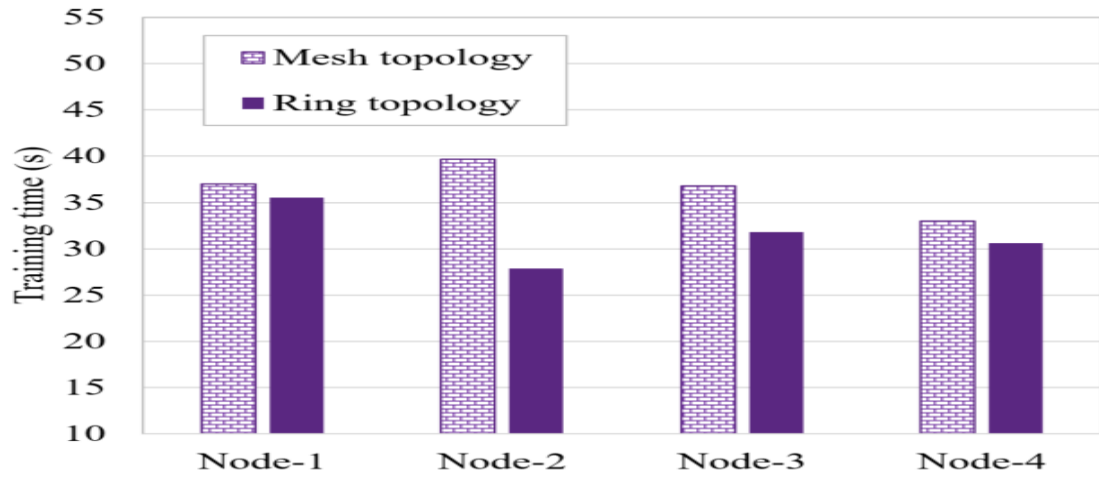


Figure 26: Training time of the local models in ring and mesh-based networks

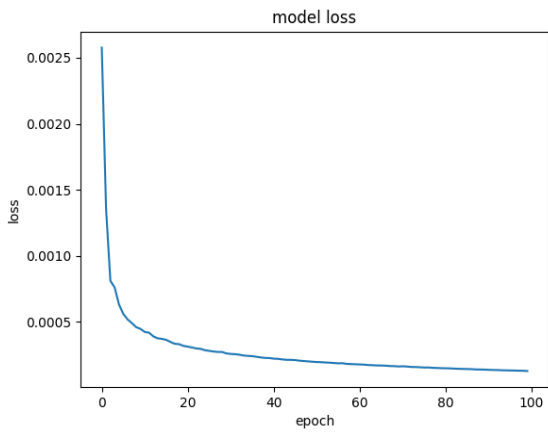


Figure 27: Global loss after using ring-based DFL framework

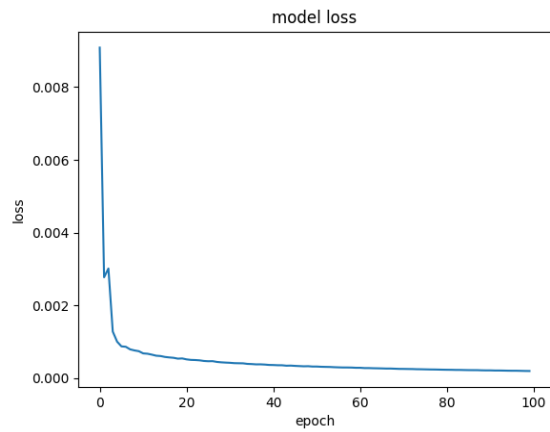


Figure 28: Global loss after using mesh-based DFL framework

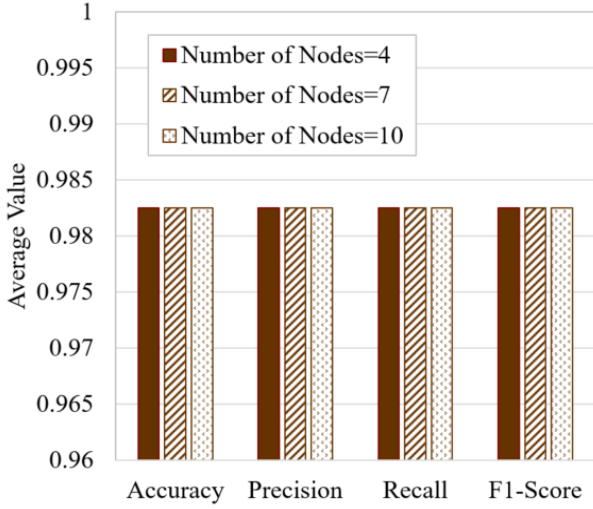


Figure 29: Average accuracy, precision, recall, and F1-Score of the local models in ring-based network

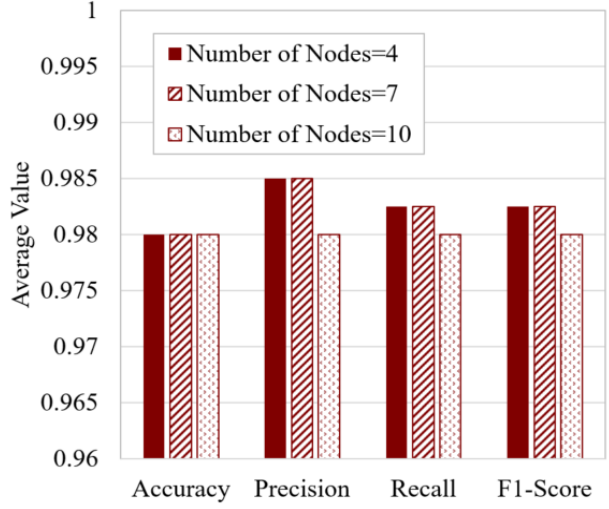


Figure 30: Average accuracy, precision, recall, and F1-Score of the local models in mesh-based network

27 and 28, respectively. As we observe from the figures, the global loss is  $<0.0005$  for ring topology and  $<0.0002$  for mesh topology, after 100 epochs. The experimental results after three rounds are presented in the figures. We observed that after 10 rounds the loss is below 0.00002 for both the ring-based and mesh-based DFL frameworks, which is almost negligible. In Section 3.3, theoretically we have already proved that the global loss tends to 0 as the number of rounds increases. Now, the experimental results also demonstrate the same.

We conducted the experiment for seven and ten nodes also. As we observed from the results, the average accuracy, precision, recall, and F1-Score were above 0.98 while using ring topology. We also observed that while using mesh topology the average accuracy, precision, recall, and F1-Score were above 0.97. However, from the results we observed that for some of the nodes ring topology provided higher accuracy and for other nodes mesh topology provided higher accuracy. However, in both the cases the average accuracy, precision, and recall, and F1-Score were above 0.97. Hence, we observed from the results that for both the ring and mesh topology, high prediction accuracy was obtained by the DFL in all three scenarios. The average accuracy, precision, recall, and F1-Score for the ring-based and mesh-based DFL frameworks are presented in Figs. 29 and 30, respectively. *The prediction accuracy of the global model developed by the nodes for the three scenarios for mesh topology and ring topology were  $\geq 0.98$ .* The average training time for the local models while using ring and mesh topology are presented in Fig. 31.

As observed from the results, the average training time of the local models for scenarios 1, 2, and 3 are 31.46 s, 32.26 s, and 30.98 s, respectively while using ring topology. We also observed that while using mesh topology, the average training time of the local models for scenarios 1, 2, and 3 are 36.6 s, 58.4 s, and 96.71 s, respectively. We observed that for both ring and mesh topology with four, seven, and ten nodes, it took two rounds to get the desired accuracy level of 0.95, and the difference between the accuracy levels attained

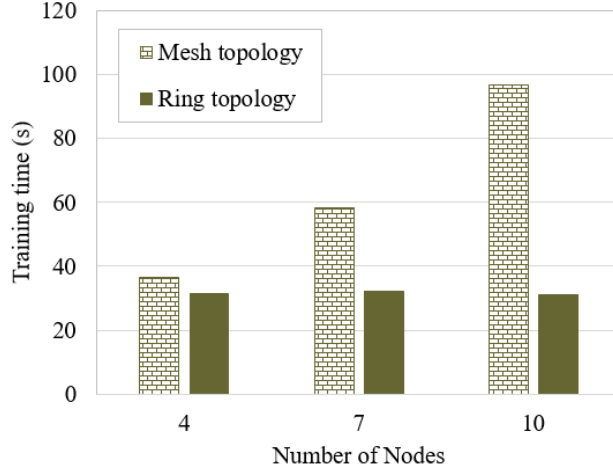


Figure 31: Average training time of the local models in ring and mesh-based networks

by two consecutive rounds was  $< 0.001$  after three rounds for each of the nodes. In ring topology, each node exchanges model updates with the adjacent nodes, whereas in mesh topology, each node exchanges model updates with rest of the nodes in the formed network. As we observed in our experiment, the training time for mesh topology was higher. We also measured the response time for both the mesh-based and ring-based networks, and we observed that for both ring and mesh topology, the response time was in the range of 1.2-3.5s, in all the three cases.

Finally we observe that (i) for CFL we achieved  $\geq 97\%$  accuracy for the global model, and (ii) for DFL using ring and mesh topology we achieved  $\geq 98\%$  and  $\geq 97\%$  prediction accuracy respectively for the local models, and  $\geq 98\%$  accuracy for the global model. As we observe from the experimental results, using CFL and DFL, high prediction accuracy can be obtained without sharing the data.

#### 4.5. Comparison with existing crop yield prediction approaches

In this section, we compare the performance of the CFL and DFL-based frameworks in crop yield prediction with the state-of-the-art models for crop yield prediction. The comparative analysis is presented in Table 4. At first, we compare the CFL and DFL-based frameworks with the existing crop yield prediction frameworks that used the *same dataset*<sup>1</sup> that we used for performance analysis. After that we draw a comparison of the CFL and DFL-based frameworks with an existing FL-based framework that used another dataset for performance evaluation.

In (Thilakarathne et al. ((2022))), the authors used RF, DT, KNN, XGBoost, and SVM, which are well-known ML models, and among them RF achieved the highest accuracy of 97.18%. In (Bakthavatchalam et al. ((2022))), MLP was used and 98.23% accuracy was achieved in crop yield prediction. KNN was adopted in (Cruz et al. ((2022))) for data analysis and an accuracy of 92.62% was achieved for crop yield prediction. In (Kathiria et al. ((2023))), the authors used DT, SVM, KNN, LGBM, and RF, in crop yield prediction,

Table 4: Comparison of performance of proposed and existing crop yield prediction frameworks

Work	Classifier	FL is used	Accuracy	Training time	Response time
Thilakarathne et al. ((2022))	RF (Highest), DT, KNN, XGBoost, SVM	No	97.18%	Not measured	Not measured
Bakthavatchalam et al. ((2022))	MLP (Highest), Decision Table, JRip	No	98.23%	Model build time: 10.56 s (MLP)	Not measured
Cruz et al. ((2022))	KNN	No	92.62% (Recall)	Not measured	Not measured
Kathiria et al. ((2023))	DT, SVM, KNN, LGBM, RF (Highest)	No	99.24%	Not measured	Not measured
Gopi and Karthikeyan ((2024))	LSTM, Bi-LSTM, GRU	No	98.45%	Not measured	Not measured
Idoje et al. ((2023))	Gaussian NB	Yes (CFL)	90%	Not measured	Not measured
FL-based framework	LSTM	Yes (CFL and DFL)	CFL: $\geq 97\%$ (global) (5-15 clients), DFL: $\geq 98\%$ (local) (Ring) (4-10 nodes), $\geq 97\%$ (local) (Mesh) (4-10 nodes), $\geq 98\%$ (global) (Mesh and ring)	CFL: 60-200 s (5-15 clients), DFL: 25-40 s (Ring) (4-10 nodes), 30-100 s (Mesh) (4-10 nodes)	CFL: 2.5-5 s (5-15 clients), DFL: 1.2-3.5 s (4-10 nodes)

and among them RF achieved the highest accuracy of 99.24%. The authors in (Gopi and Karthikeyan ((2024))) used LSTM, Bi-LSTM, and GRU-based framework for data analysis, and achieved an accuracy of 98.45% in crop yield prediction. As we observe from Table 4, none of the existing approaches used FL. Most of the existing approaches focused on the use of ML/DL approaches for crop yield prediction without addressing the concern of using cloud-only paradigm for data analysis, such as network connectivity issue, data privacy, response time, etc. To achieve data privacy protection by without sharing data but obtain a model with high prediction accuracy through collaborative training has been addressed in our work. We have explored the use of FL in crop yield prediction through an experimental analysis using multiple clients. As we observe CFL and DFL have achieved  $\geq 97\%$  prediction accuracy but without sharing actual datasets. Hence, we observe that using FL high prediction accuracy can be obtained like the state-of-the-art models but with enhanced data privacy. In (Idoje et al. ((2023))), CFL was used for crop yield prediction based on Gaussian NB, and 90% prediction accuracy was achieved with Adam optimizer and learning rate 0.001. As we observe, only CFL was used in (Idoje et al. ((2023))), whereas we have used both CFL and DFL in crop yield prediction based on LSTM. Further, we have achieved higher accuracy ( $\geq 97\%$ ) than (Idoje et al. ((2023))) (Optimizer: Adam, learning rate: 0.001). Further, the training time for both the CFL and DFL approaches have been determined in our work, and we observe that the training time is medium for the considered scenarios. We also observe that the response time is low for both the CFL and DFL-based strategies. Thus, crop yield prediction with high accuracy but low response time can be achieved using FL-based frameworks.

## 5. Future Research Directions

In this work, we have concentrated on the use of CFL and DFL in crop yield prediction. However, there still remains several challenges stated as follows.

- **Data heterogeneity:** Data heterogeneity is a critical issue of FL. As the data is distributed among several clients, it may lead to non-independent and identically distributed and unbalanced datasets. In such a scenario, model training is a challenge and it becomes critical to build a global model with consistent performance across all the clients.
- **Use of FTL:** The datasets of different clients may have different sample space as well as different feature space. In that case, FTL can be used. In FTL, features from different feature spaces are transferred to the same presentation. Further, for enhancing data privacy and security, gradient updates are encrypted. The use of FTL with gradient encryption in crop yield prediction is a significant research direction.
- **Resource limitation of user device:** The FL encourages local data analysis and collaborative learning. However, the user device may not have sufficient resources for executing an ML/DL algorithm, and the user has to use the cloud server for data analysis. Another difficulty may arise when a device cannot execute its local model



due to resource limitation or any other issue. In that case, the model of that device along with the dataset needs to be transferred to a nearby node. In both the scenarios, cryptography or steganography can be used for protecting the data privacy by either encrypting or hiding it inside a media during transmission.

- Enhance security of model parameters and the system: Though, no data is shared and the model updates are exchanged in FL, still there is a possibility of leakage of gradient information. In such a scenario, gradient encryption can be used. Further, blockchain can be integrated with FL for enhancing the security of the entire system.
- Communication overhead: In FL, the exchange of model updates during training enhances the communication overhead and latency. Therefore, a trade-off should be maintained between the number of rounds of training the model and communication overhead, so that prediction accuracy can be good but the latency will not be very high.

## 6. Conclusions

Crop yield prediction is a crucial area of smart agriculture. In this paper, we have explored the use of CFL and DFL in crop yield prediction based on LSTM. An experimental case study has been conducted, where different number of devices perform collaborative training using CFL and DFL. To implement CFL, a client-server paradigm is developed using MSocket, and multiple clients are handled by the server. To implement the DFL, a collaborative network is formed using ring topology and mesh topology. In the ring-based P2P network, each node exchanges model updates with the neighbour nodes and performs aggregation to build the upgraded model. In the mesh-based network, each node exchanges model updates with rest of the nodes and performs aggregation to build the upgraded model. The performance of the CFL and DFL-based frameworks are evaluated in terms of prediction accuracy, precision, recall, F1-Score, and training time. The experimental results present that  $\geq 97\%$  prediction accuracy has been achieved using the CFL and DFL-based frameworks. The results also show that the CFL-based framework reduces the response time  $\sim 75\%$  than the cloud-only framework. The average accuracy, precision, recall, and F1-Score are also improved by  $\sim 5\%$ ,  $\sim 7\%$ ,  $\sim 8\%$ , and  $\sim 9\%$  using CFL than the cloud-only framework. Finally, the future research directions in crop yield prediction are highlighted in this paper.

## Acknowledgements

This work is partially supported by An ARC Discovery Project (DP240102088).

## References

- S. B. Atitallah, M. Driss, and H. B. Ghezala. Fedmicro-ida: A federated learning and microservices-based framework for iot data analytics. *Internet of Things*, 23:100845, 2023.

- K. Bakthavatchalam, B. Karthik, V. Thiruvengadam, S. Muthal, D. Jose, K. Kotecha, and V. Varadarajan. Iot framework for measurement and precision agriculture: predicting the crop using machine learning algorithms. *Technologies*, 10(1):13, 2022.
- S. Bera, T. Dey, S. Ghosh, and A. Mukherjee. Internet of things and dew computing-based system for smart agriculture. In *Dew Computing: The Sustainable IoT Perspectives*, pages 289–316. Springer, 2023a.
- S. Bera, T. Dey, A. Mukherjee, and R. Buyya. E-cropreco: a dew-edge-based multi-parametric crop recommendation framework for internet of agricultural things. *The Journal of Supercomputing*, 79(11): 11965–11999, 2023b.
- S. Bera, T. Dey, A. Mukherjee, and D. De. Flag: Federated learning for sustainable irrigation in agriculture 5.0. *IEEE Transactions on Consumer Electronics*, 70(1):2303–2310, 2024.
- A. D. Boursianis, M. S. Papadopoulou, P. Diamantoulakis, A. Liopa-Tsakalidi, B. Pantelis, G. Salahas, G. Karagiannidis, S. Wan, and G. S. K. Internet of things (iot) and agricultural unmanned aerial vehicles (uavs) in smart farming: a comprehensive review. *Internet of Things*, 18:100187, 2022.
- M. Cruz, S. Mafra, and E. Teixeira. An iot crop recommendation system with k-nn and lora for precision farming. 2022.
- O. Debauche, J.-P. Trani, S. Mahmoudi, P. Manneback, J. Bindelle, S. A. Mahmoudi, A. Guttadauria, and F. Lebeau. Data management and internet of things: A methodological review in smart farming. *Internet of Things*, 14:100378, 2021.
- T. Dey, S. Bera, B. Paul, D. De, A. Mukherjee, and R. Buyya. Fly: Femtolet-based edge-cloud framework for crop yield prediction using bidirectional long short-term memory. *Software: Practice and Experience*, 54(8):1361–1377, 2024.
- Y. Djenouri, T. P. Michalak, and J. C.-W. Lin. Federated deep learning for smart city edge-based applications. *Future Generation Computer Systems*, 147:350–359, 2023.
- A. Durrant, M. Markovic, D. Matthews, D. May, J. Enright, and G. Leontidis. The role of cross-silo federated learning in facilitating data sharing in the agri-food sector. *Computers and Electronics in Agriculture*, 193:106648, 2022.
- O. Friha, M. A. Ferrag, L. Shu, L. Maglaras, K.-K. R. Choo, and M. Nafaa. Felids: Federated learning-based intrusion detection system for agricultural internet of things. *Journal of Parallel and Distributed Computing*, 165:17–31, 2022.
- P. M. Gopal and R. Bhargavi. A novel approach for efficient crop yield prediction. *Computers and Electronics in Agriculture*, 165:104968, 2019.
- P. Gopi and M. Karthikeyan. Red fox optimization with ensemble recurrent neural network for crop recommendation and yield prediction model. *Multimedia Tools and Applications*, 83(5):13159–13179, 2024.
- G. Idoje, T. Dagiuklas, and M. Iqbal. Federated learning: Crop classification in a smart farm decentralised network. *Smart Agricultural Technology*, 5:100277, 2023.
- P. Kathiria, U. Patel, S. Madhwani, and C. Mansuri. Smart crop recommendation system: A machine learning approach for precision agriculture. In *Machine Intelligence Techniques for Data Analysis and Signal Processing: Proceedings of the 4th International Conference MISIP 2022, Volume 1*, pages 841–850. Springer, 2023.
- A. Li, M. Markovic, P. Edwards, and G. Leontidis. Model pruning enables localized and efficient federated learning for yield forecasting and data sharing. *Expert Systems with Applications*, 242:122847, 2024.
- L. Li, Y. Fan, M. Tse, and K.-Y. Lin. A review of applications in federated learning. *Computers & Industrial Engineering*, 149:106854, 2020.
- T. Manoj, K. Makkithaya, and V. Narendra. A federated learning-based crop yield prediction for agricultural production risk management. In *Proceedings of the 2022 IEEE Delhi Section Conference (DELCON)*, pages 1–7. IEEE, 2022.
- V. Mothukuri, R. M. Parizi, S. Pouriyeh, Y. Huang, A. Dehghantanha, and G. Srivastava. A survey on security and privacy of federated learning. *Future Generation Computer Systems*, 115:619–640, 2021.
- D. C. Nguyen, M. Ding, P. N. Pathirana, A. Seneviratne, J. Li, and H. V. Poor. Federated learning for internet of things: A comprehensive survey. *IEEE Communications Surveys & Tutorials*, 23(3):1622–1658, 2021.

- N. N. Thilakarathne, M. S. A. Bakar, P. E. Abas, and H. Yassin. A cloud enabled crop recommendation platform for machine learning-driven precision farming. *Sensors*, 22(16):6299, 2022.
- T. Van Klompenburg, A. Kassahun, and C. Catal. Crop yield prediction using machine learning: A systematic literature review. *Computers and electronics in agriculture*, 177:105709, 2020.
- C. Zhang, Y. Xie, H. Bai, B. Yu, W. Li, and Y. Gao. A survey on federated learning. *Knowledge-Based Systems*, 216:106775, 2021.
- W. Zhu, M. Goudarzi, and R. Buyya. Flight: A lightweight federated learning framework in edge and fog computing. *Software: Practice and Experience*, 54(5):813–841, 2024.